

Autonomous Flight Control for a Planetary Exploration Aerobot

Alberto Elfes¹, James F. Montgomery¹, Jeffery L. Hall¹, Sanjay S. Joshi², Jeffrey Payne²,
Charles F. Bergh¹

¹Jet Propulsion Laboratory, Pasadena, CA 91109, USA. Email: {elfes, monty, jeffery.l.hall, cfb}@jpl.nasa.gov

²University of California, Davis, California 95616, USA. Email: {maejoshi, jwpayne}@ucdavis.edu

Robotic lighter-than-air vehicles, or aerobots, provide a strategic platform for the exploration of planets and moons with an atmosphere, such as Venus, Mars, Titan and the gas giants. Aerobots have modest power requirements, extended mission duration and long traverse capabilities. They can execute regional surveys, transport and deploy scientific instruments and in-situ laboratory facilities over vast distances, and also provide wide-area surface sampling. With the arrival of the Huygens probe at Saturn's moon Titan on January 14, 2005, there is considerable interest in a follow-on mission that would use a substantially autonomous aerobot to explore Titan's surface. In this paper, we discuss steps towards the development of an autonomy architecture, and concentrate on the autonomous flight control subsystem. Two research directions are described: first, the development of a highly accurate aerodynamic airship model and its validation; second, an initial implementation of the flight control system and the results obtained from autonomous flight tests conducted in the Mojave desert. We conclude by outlining further issues for research.

I. Introduction

Exploration of the planets and moons of the Solar System has up to now relied on remote sensing from Earth, fly-by probes, orbiters, landers and rovers. Remote sensing probes and orbiters can only provide non-contact, limited resolution imagery over a small number of spectral bands; landers provide high-resolution imagery and in-situ data collection and analysis capabilities, but only for a single site; while rovers allow imagery collection and in-situ science across their path. The fundamental drawback of ground-based systems is limited coverage: in past or planned exploration missions, the rover range has varied from approximately 130m for the 1997 Sojourner mission, to currently 4.0 km for the Mars Exploration Rovers, to tens of kilometers for the teleoperated Lunokhod rovers.

There is currently a strategic gap in robotic exploration technologies for systems that combine extensive geographical coverage with high-resolution data collection and in-situ science capabilities. For planets and moons with an atmosphere, this gap can be addressed through aerial vehicles. In the Solar System, in addition to Earth, the planets Venus and Mars, the gas giants (Jupiter, Saturn, Uranus and Neptune) and the Saturn moon Titan have significant atmospheres. Aerial vehicles that have been considered for planetary exploration include airplanes and gliders, helicopters, balloons [Kerzhanovich 2002] and airships. Flight time for gliders depends heavily on wind and updraft patterns, which in turn constrain their surface coverage, while airplanes and helicopters expend significant energy resources simply staying airborne [Elfes 2001, Elfes 2003].

The NASA 2003 Solar System Exploration Roadmap identifies aerial vehicles as strategic platforms for the exploration of Mars, Venus and Titan [NASA 2003]. It also defines advanced autonomy technologies as a high priority development area for the operation of aerial exploration vehicles. In this paper, we discuss the advantages and challenges involved in aerobot exploration of Titan and the required autonomy capabilities. We provide an outline of the aerobot autonomy architecture under development, and describe the JPL aerobot testbed. We also discuss the development of a highly accurate aerodynamic airship model and its validation, as well as an initial implementation of the flight control system and the results obtained from autonomous flight tests conducted in the Mojave desert.

II. Aerobots for Planetary Exploration

Lighter-than-atmosphere (LTA) systems provide significant advantages for planetary exploration due to their potential for extended mission duration, long traverse, and extensive surface coverage capabilities. Robotic airships, in particular, are ideal platforms for airborne planetary exploration. Airships have modest power requirements, and combine the extended airborne capability of balloons with the maneuverability of airplanes or helicopters. Their controllability allows precise flight path

execution for surveying purposes, long-range as well as close-up ground observations, station-keeping for long-term monitoring of high-value science sites, transportation and deployment of scientific instruments and in-situ laboratory facilities across vast distances to key science sites, and opportunistic flight path replanning in response to the detection of relevant science sensor signatures. Furthermore, robotic airships provide the ability to conduct extensive surveys over both solid terrain and liquid-covered areas, and to reconnoiter sites that are inaccessible to ground vehicles.

Implementation of these capabilities requires achieving a high degree of vehicle autonomy across a broad spectrum of operational scenarios. An integrated set of enabling technologies for autonomous aerobot navigation and aerial exploration is currently not available, and is the core focus of the research being developed at JPL by the authors [Hall 2002a, Hall 2004, Elfes 2003, Elfes 2004].

III. Saturn's Moon Titan

NASA's 2003 Solar System Exploration Roadmap specifies a follow-on Titan mission with an *in-situ* vehicle as a high priority after the Cassini-Huygens mission. Titan is the largest moon of Saturn, with a radius of 2,575 km. It has an atmosphere with a surface density of 5.55 kg/m³ (4.6 times the density of the Earth's atmosphere at sea level), and an estimated composition of 95% nitrogen, 3% methane and 2% argon. The surface pressure is approximately 1.5 bar, and the gravity at the surface is 1.35 m/s² (1/7 of the gravity of Earth). The surface temperature is approximately -180° C.

The upper atmosphere of Titan has a thick haze, caused by sunlight-induced chemical reactions of methane, which shrouds the surface of Titan from visual observation (Fig. 1). As a result, very little is known of Titan's geography and geology. Early Voyager fly-by observations and recent Hubble Space Telescope (HST) images in the near-infrared spectrum (0.85 to 1.05 microns) indicated the possible existence of continental masses composed of solid rock and frozen water ice, and of liquid bodies potentially composed of liquid ethane and methane [Hall 2002a, Hall 2002b, Lorenz 2000]. Additional long-term observations have also provided indications of weather on Titan, including clouds and storms.

The successful descent of the Huygens probe to the surface of Titan on January 14, 2005 has provided spectacular images of a very complex terrain (Fig. 2). While the data is still in the early stages of processing and analysis, and much will be learned in the coming months, it is clear that many scientific questions will remain unanswered, particularly in the areas of weather and seasonal variability, subsurface morphology, and the composition and distribution of surface organic material [Chyba 1999], leading to the requirement for a follow-on mission.

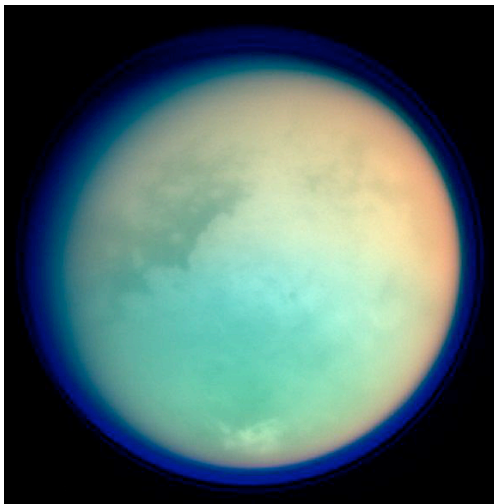


Fig. 1: False-color image of Titan, using ultraviolet and infrared images taken by Cassini's imaging science subsystem on Oct. 26, 2004. Red and green colors represent infrared wavelengths and show areas where atmospheric methane absorbs light. These colors reveal a brighter (redder) northern hemisphere. Blue represents ultraviolet wavelengths and shows the high atmosphere and detached hazes. Bright surface areas indicate continental masses, while dark areas may indicate regions with liquid methane and ethane or basins of deposited material. Source: NASA/JPL/Space Science Institute, ref. PIA06139.

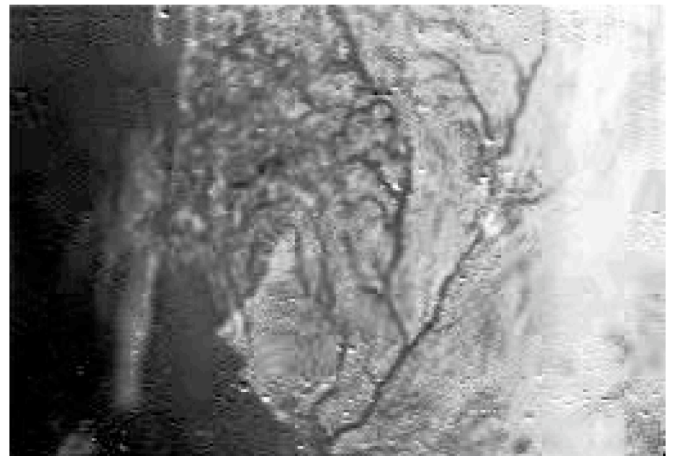


Fig. 2: Titan surface image taken by the Huygens probe during descent. It was taken at an altitude of 16.2 km, with a resolution of approximately 40 m/pixel. An early interpretation suggests the presence of a drainage system in the "highlands" (lighter areas) that leads into a darker region that may be a basin of deposited hydrocarbons. Methane clouds and what may be a methane/ethane fog close to the "shore" can be seen. Source: ESA/NASA/JPL/University of Arizona.

IV. Aerobot Autonomy Architecture

The main challenges for aerobot exploration of Titan include: *large communication latencies*, with a round trip light time of approximately 2.6 hours; *extended communication blackout periods* with a duration of up to 9 Earth days, caused by the rotation of Titan and its orbital occlusion by Saturn; *extended mission duration*, currently projected to be on the order of six months to one year; and *operation in substantially unknown environments*, with largely unknown wind patterns, meteorological conditions, and surface topography.

These challenges impose the following capability requirements on a Titan aerobot: *vehicle safing*, so that the safety and integrity of the aerobot can be ensured over the full duration of the mission and during extended communication blackouts; *accurate and robust autonomous flight control*, including deployment/lift-off, long traverses, hovering/station-keeping, and touch-and-go surface sampling; *spatial mapping and self-localization* in the absence of a global positioning system and probably of a magnetic field on Titan; and *advanced perceptual hazard and target recognition, tracking and servoing*, allowing the aerobot to detect and avoid atmospheric and topographic hazards, and also to identify, home in, and keep station over pre-defined science targets or terrain features. We have discussed elsewhere a broad range of mission scenarios and identified the associated autonomy requirements [Hall 2002b].

To address the aerobot autonomy capabilities required above, we are developing an aerobot autonomy architecture that integrates accurate and robust vehicle and flight trajectory control, perception-based state estimation, hazard detection and avoidance, vehicle health monitoring and reflexive safing actions, vision-based localization and mapping, and long-range mission planning and monitoring (Fig. 3).

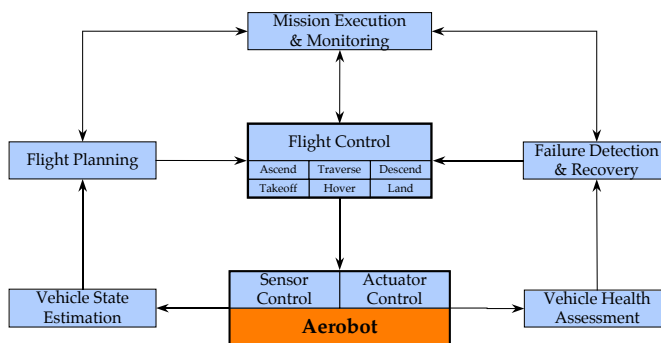


Fig. 3: Aerobot autonomy architecture with major subsystems.

Lower level functions in the autonomy architecture include sensor and actuator control, vehicle state estimation, flight mode control, supervisory flight control, and flight profile execution. Intermediate level functions include vehicle health monitoring, failure detection and recovery, flight trajectory and profile planning, and vision based navigation. The latter provides GPS-independent localization, local and regional mapping, and hazard detection and avoidance (HDA) capabilities. Higher-level functions include mission planning, resource management, and mission execution and monitoring.

The research discussed in this paper concentrates on the actuator and vehicle flight control subsystems. This includes development of a robust flight control system based on vehicle aerodynamic modeling, system simulation for robust control law development and testing, and vehicle system identification; and of accurate vehicle multi-sensor state estimation methods, using both inertial and vision-based motion and position estimation. In the discussion below, we describe in more detail our work on the flight control system.

V. Aerobot Aerodynamic Modeling and Validation

The aerobot flight control system being developed is based on: (1) system modeling, which includes aerodynamic, airship sensor and actuator, and environmental modeling; (2) system identification for aerodynamic parameter estimation; (3) model and control system validation in a physically based simulation environment; and (4) flight testing on the aerobot testbed.

The aerodynamic model developed for the JPL airship is significantly different from fixed-wing or rotary-wing aircraft aerodynamic models, as the virtual mass and inertia properties of the displaced atmospheric volume are substantial when compared with those associated with the vehicle itself. Additionally, an aerobot is characterized by having different flight modes (take-off/landing, station-keeping/hovering, loitering, ascent/descent, high-speed cruise, low-speed flight) that require alternative actuator control strategies and flight control algorithms. Important airship flight control challenges include non-minimum phase behavior and oscillatory modes at low speeds, time-varying behavior due to altitude variations, and variable efficiency of the actuators depending on aerobot speed [Gomes 1990, Elfes 2001].

We developed a new nonlinear robotic airship model intended for control system design and evaluation. The model brings together much of the previous airship modeling results available in the literature, and adds new elements to extend the model's range of applicability. In addition, it is built from a systems-design-control interaction perspective, in which physical elements are parameterized to easily make design changes as control systems are designed and evaluated. The kinematic and dynamic equations of the model are discussed in [Payne 2004], and are not repeated here due to space constraints.

The aerodynamic model developed has the ability to simulate all four primary modes of flight (launch, cruise, hover, landing). It has been programmed using the ADAMS 12.0 modeling software, which provides the ability to implement the equations of motion automatically, create detailed animations, and interface with Simulink. In order to make the model as versatile as possible for changing flight conditions and optimization studies, all ship dimensions are given parametric definitions. The reference frame for the airship is the hull center of volume and is defined using a North-East-Down orientation, as is typically done with aircraft (Fig. 4).

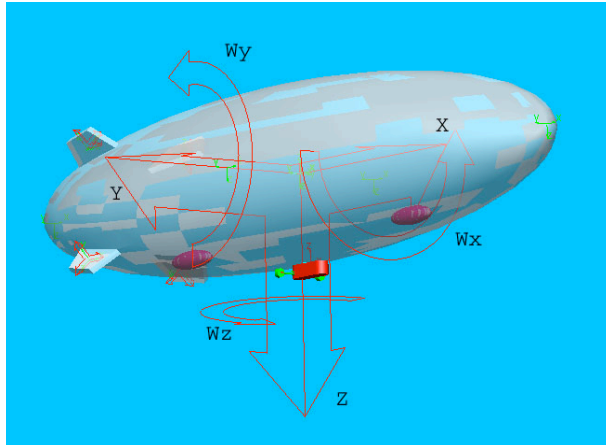


Fig. 4: Aerodynamic model and coordinate system.

In order to verify the accuracy of the model, various simulations were run and the results compared to expectation and experience. We summarize below some of the results; a complete description of the model, a more extensive set of validation experiments, and the corresponding results are found in [Payne 2004].

A. Forward Motion

Both thrusters were given a step input of 4 N with zero angle relative to the ship; the fins had zero deflection. The ship had $V_0 = 0$ and started at an elevation of 5m. As expected, the ship initially pitches upward as it loses altitude (Fig. 5). The pitch upward is due to the step input to the engines whereas the heaviness condition (negative buoyancy) of the vehicle causes the drop in elevation. As the ship gains speed, the pitch angle begins oscillating about a positive value, creating aerodynamic lift as verified in field conditions.

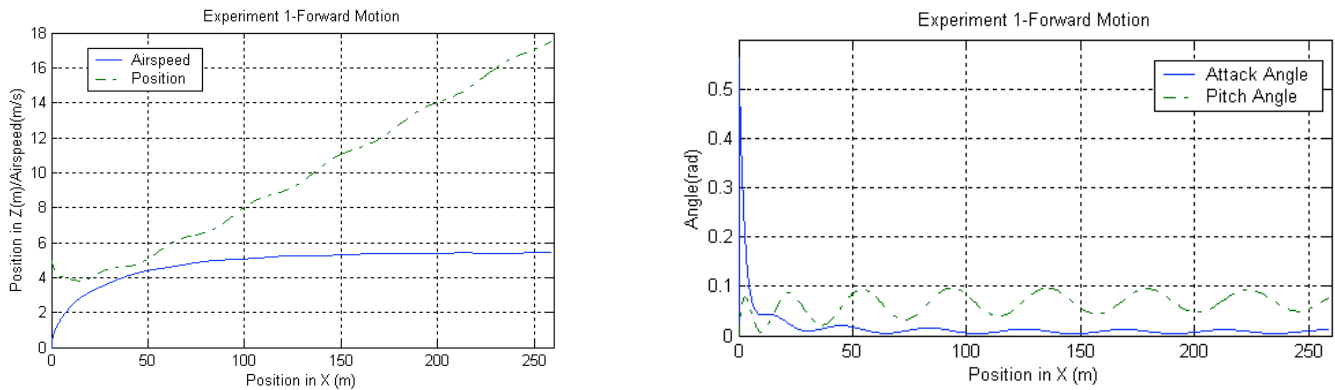


Fig. 5. Aerodynamic model flight test, showing forward motion and attack and pitch angles.

B. Rudder Test

Control surface behaviour was tested by inputting a -20° deflection angle and repeating the previous test. The angle represents the deflection of the upper port and upper starboard fins about their center axis. As previously described, the opposing fins are rigidly coupled. This results in a negative slip angle that moves the airship to port. The trajectory in the XY plane gradually converges to a circle (Fig. 6(a)). This is also shown in Fig. 6(d), where the slip angle derivative approaches zero. In the XZ plane (Fig. 6(b)), the ship gains altitude due to the upward pitch, as discussed before.

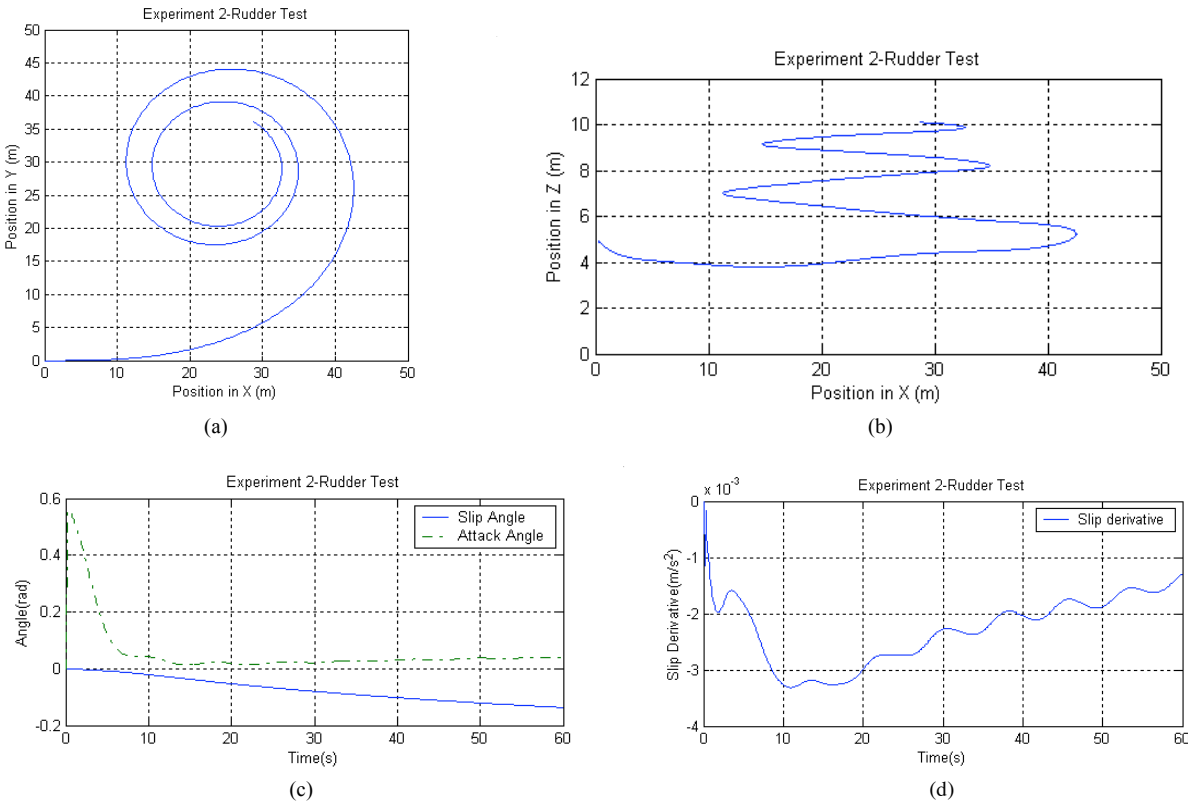


Fig. 6: Control surface deflection resulting in limit cycle flight trajectory.

VI. The JPL Aerobot Testbed

The prototype aerobot testbed developed at JPL is based on an Airspeed Airship AS-800B (Fig. 7). The airship specifications are: length of 11 m, diameter of 2.5 m, total volume of 34 m^3 , two 2.3 kW (3 hp) 23 cm^3 (1.4 cu inch) fuel engines, double catenary gondola suspension, control surfaces in an "X" configuration, maximum speed of 13 m/s (25 kts), maximum ceiling of 500 m, average mission endurance of 60 minutes, static lift payload of 12 kg ASL, and dynamic lift payload of up to 16 kg ASL. The avionics and communication systems are installed in the gondola.

The aerobot avionics system is built around a dual PC-104+ computer architecture. One of the PC-104+ stacks is used for navigation and flight control, while the other is dedicated to image processing. The navigation stack also has a serial board interface to the navigation sensors and pan/tilt unit, a timer/counter board for reading pulse width modulated (PWM) signals from a human safety pilot and generating PWM signals based upon control surface commands from the avionics software, and an IEEE 1394 board for sending commands to, and reading image data from, the navigation and science cameras. The perception processor is dedicated to image processing and image-based motion estimation (IBME). Wireless serial modems provide data/control telemetry links between the aerobot and the ground station, and additional video transmitters on the aerobot provide downlinks of video imagery to the ground station. The safety pilot can always reassert "pilot override" control over the aerobot.

The navigation sensors currently consist of an IMU (angular rates, linear accelerations), a compass/inclinometer (yaw, roll and pitch angles) and DGPS (for absolute 3D position). The vision sensors include two down-looking navigation cameras, one with a $360^\circ \times 180^\circ$ field of view and another with a narrower FOV. Additionally, we plan to integrate a laser altimeter (surface relative altitude), a barometric altimeter (absolute altitude against reference point), an ultrasonic anemometer (3D wind speed), and a science camera mounted on a pan/tilt unit.



Fig. 7: Autonomous flight of the JPL aerobot, conducted at the El Mirage dry lake in the Mojave desert. The JPL aerobot testbed has a length of 11 m, a diameter of 2.5 m, and a static lift payload of approximately 12 kg.

The ground station is composed of a laptop, a graphical user interface to the vehicle, wireless data and video links, video monitors and VCRs, and a differential GPS (DGPS) base station that provides differential corrections to the GPS receiver onboard the aerobot, allowing vehicle 3D position estimates with an accuracy on the order of centimeters. Field tests of the JPL aerobot are conducted at the El Mirage dry lake site in the Mojave desert. Initial flights were teleoperated to allow extensive testing of the onboard avionics systems.

VII. Autonomous Flight Control

The flight control system has a layered supervisory control structure (Fig. 8). It oversees the main flight trajectory modes (cruise, hover and loiter), which use ascent, descent, turn and altitude controllers. These in turn command the vehicle attitude and thrust controllers. For an “X-tail” configuration, the opposing tail surfaces (1+3 and 2+4) are operated in a coupled mode. This means there is no direct roll control, and also that “pure” elevator and rudder behaviour is implemented through actuation of all four control surfaces.

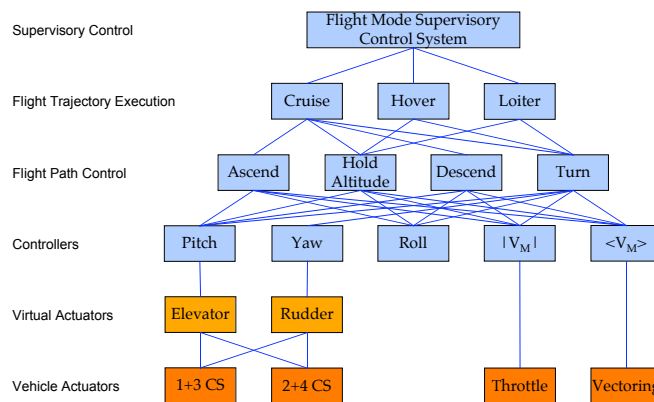


Fig. 8: Layered supervisory control structure of the aerobot flight control system. “CS” stands for the tail control surfaces, which are arranged in an “X” or ruddervator configuration.

Over the past 12 months, we have initiated testing of the onboard flight autonomy system. The first version has been implemented using PI controllers for pitch, yaw and altitude control and corresponds to the “controller” and “flight path control” levels in the supervisory control architecture (Fig. 8). We have chosen this implementation path because it allowed us to quickly initiate autonomous flight tests, capitalize on our previous work in autonomous helicopter control, and gain additional field test experience concerning aerobot dynamics and behaviour under varying atmospheric and wind conditions.

Since the full aerodynamic model and the associated simulation tools are now operational, we plan to transition to a set of robust controllers, which we expect will demonstrate tighter vehicle control and more accurate trajectory control under wind disturbances.

A. Yaw, Pitch and Altitude Control

Below we present some example results from our autonomous flight tests, conducted at the El Mirage test site. The performance of the yaw (direction) controller is shown in Fig. 9. As can be seen, the vehicle has a fast response to yaw commands, and the yaw controller overshoot is small.

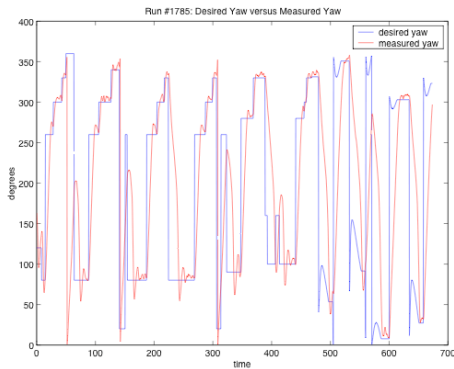


Fig. 9: Autonomous yaw control. Commanded yaw is shown in blue, while measured yaw is shown in red. Note that the measured yaw sometimes shows a plotting artifact, as it suffers a wrap-around from 360° to 0° .

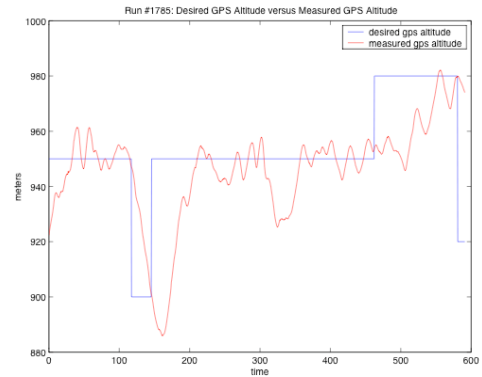


Fig. 10: Autonomous altitude control. Commanded altitude is shown in blue, while measured altitude is shown in red.

Fig. 10 shows the performance of the altitude controller, which in turn uses the pitch controller. Pitch and, correspondingly, altitude control show significantly higher oscillation, which is intrinsic to the dynamics of the vehicle (section V). In fact, some of the key airship flight control challenges include non-minimum phase behavior and oscillatory modes at low speeds [Gomes 1990, Elfes 2001]. The latter is caused by the pendulum behaviour of the airship, caused by the center of gravity (CG) being located below the center of buoyancy (CB).

We are currently working on performance improvement for the yaw and the altitude/pitch controllers, both through adaptive adjustment of the PI and PID weight terms, and through the incorporation of a pitch rate controller, which can be used to actively control and reduce the oscillatory pitch behaviour of the aerobot.

B. Waypoint Flight Control

At the flight trajectory execution control level in the supervisory control architecture (Fig. 8), we have implemented a waypoint flight control system. Waypoints are specified by the operator, who also sets the satisficing conditions that define when a waypoint has been considered reached. The approach used is called “orienting”, where the control objective is defined in terms of reaching the waypoint, rather than in terms of the deviation from a given trajectory. Figs. 11 – 13 show autonomous waypoint flight control tests, again conducted at El Mirage.

Fig. 11 shows waypoint flight control for a sequence of 3 waypoints. A waypoint is specified as having been reached if the aerobot is within an Euclidean distance of 25m from the GPS waypoint coordinates. A more complex test is shown in Fig. 12, where a total of 6 waypoints are visited. Atmospheric conditions for both flights were moderate, with winds speeds below 5 knots. Finally, Fig. 13 shows an autonomous flight test under substantial wind conditions, with gusts up to 10 knots. The airship is blown off the direct waypoint route on several occasions when it is in a beam reach (orthogonal) condition relative to the wind direction. Additionally, it is occasionally yawed off course when heading into or crossing the wind. Nevertheless, the autonomous flight control system was able, even under these severe wind disturbances, to visit all waypoints. We plan to address wind disturbances explicitly through the incorporation of an H_∞ robust controller design [Elfes 2001].

Pose (position and orientation in 6 DOF) and motion estimation is currently done by fusion of IMU and GPS data using a Kalman filter, allowing assessment of the vehicle flight control and trajectory following accuracy. To achieve global and regional localization on Titan in a GPS-independent manner, we are both investigating a celestial body tracker for ephemerides-based global position estimates, and developing an image-based motion estimation (IBME) system with an associated multi-sensor state estimation filter that will be used to fuse inertial and visual navigation estimates [Roumeliotis 2002].

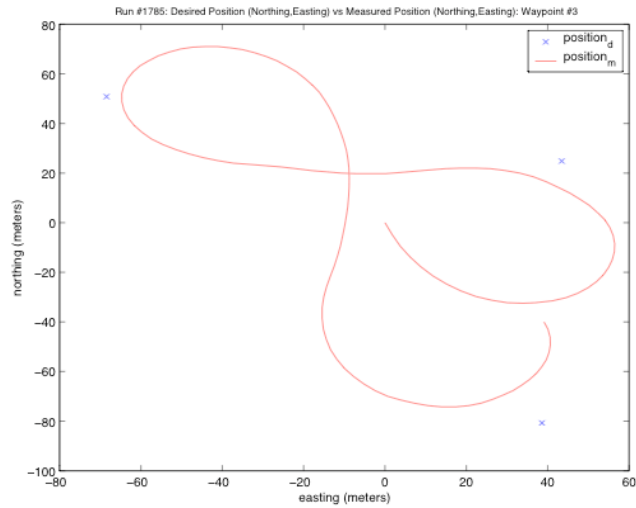


Fig. 11: Waypoint flight control. Three waypoints have been reached, with an operator-defined threshold of 25m to the GPS coordinates of the target.

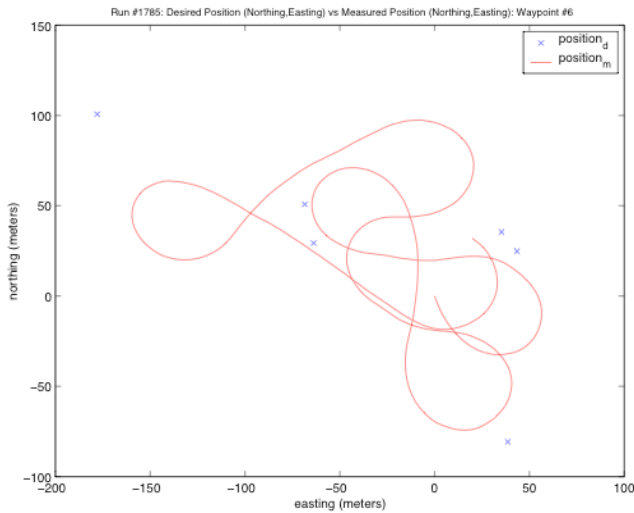


Fig. 12: Waypoint flight control. A total of 6 waypoints have been visited.

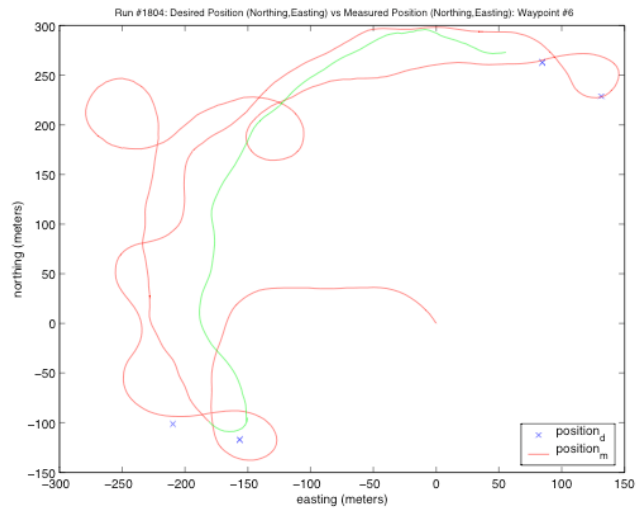


Fig. 13: Waypoint flight control under severe wind disturbances. All waypoints were reached.

VIII. Conclusions

LTA systems are a strategic platform for the exploration of planets and moons with an atmosphere, such as Venus, Mars and Titan. Aerobots, in particular, can provide geographically extensive science data at high resolutions and over varied terrains to a degree that cannot be matched by surface-bound rovers or other aerial vehicles. At the same time, operation of an aerobot at Titan or other destination in the solar system imposes significant long-term autonomy requirements.

The core autonomy technology needed for an aerobot mission elsewhere in the solar system is highly autonomous and robust flight control under little-known conditions. We outlined above a architecture for a substantially autonomous aerobot, described the current JPL aerobot testbed, and discussed initial steps towards the development of an aerobot flight control systems. This includes a new nonlinear robotic airship (aerobot) model intended for control system design and evaluation. The model brings together much of the airship modeling results published in the literature, and adds new features to extend the model's range of applicability. The model has been implemented, can be used to investigate all four modes of flight (launch, cruise, hover, landing) and is parametrically defined for easy design configuration.

Our next steps include improving the flight control system robustness and accuracy, developing a trajectory following system for systematic surveys, and incorporating vision-based localization and navigation capabilities.

Acknowledgments

The authors would like to acknowledge the help and support of Eric A. Kulczycki, who was instrumental in aerobot propulsion and flight testing, and Lee Magnone and Michael S. Garrett, for support in avionics system development and field testing. The research described in this paper was performed at the Jet Propulsion Laboratory, California Institute of Technology, under a contract with the National Aeronautics and Space Administration (NASA), and administered through the Intelligent Systems (IS) Program. The views and conclusions contained in this document are those of the authors and should not be interpreted as representing the official policies, either expressed or implied, of the sponsoring organizations.

References

- [Balaram 2002] J. Balaram et al. "DSEND - A High-Fidelity Dynamics and Spacecraft Simulator for Entry, Descent and Surface Landing", *IEEE 2002 Aerospace Conf.*, Big Sky, Montana, March 2002.
- [Biesiadecki 1997] J. Biesiadecki, A. Jain, M. L. James. "Advanced Simulation Environment for Autonomous Spacecraft", in *International Symposium on Artificial Intelligence, Robotics and Automation in Space (i-SAIRAS'97)*, Tokyo, Japan, July 1997.
- [Boschma 1993] J. H. Boschma. "The Development Progress of the U.S. Army's SAA LITE Unmanned Airship". In *Proceedings of the AIAA Lighter-than-Air Systems Technology Conference*, AIAA, September 1993.
- [Chyba 1999] C. Chyba et al, "Report of the Pre-biotic Chemistry in the Solar System Campaign Science Working Group", Technical Report, JPL, 1999.
- [Elfes 2001] A. Elfes et al. "Perception, Modelling and Control for an Autonomous Robotic Airship". In H. I. Christensen, G. D. Hager (eds.), *Sensor Based Intelligent Robots*, Springer-Verlag, Berlin, 2001.
- [Elfes 2003] A. Elfes et al. "Robotic Airships for Exploration of Planetary Bodies with an Atmosphere: Autonomy Challenges". *Journal of Autonomous Robots*, v. 14, n. 2/3. Kluwer Academic Publishers, The Netherlands, 2003.
- [Elfes 2004] A. Elfes, J. L. Hall, J. F. Montgomery, C. F. Bergh and B. A. Dudik. Towards a Substantially Autonomous Aerobot for Exploration of Titan. In *Proceedings of the International Conference on Robotics and Automation (ICRA 2004)*, IEEE, Las Vegas, May 2004.
- [Foster 2003] N. Foster. Airspeed Airships. <http://www.airspeedairships.com>, 2003.
- [Gomes 1990] S. B. V. Gomes. "An Investigation of the Flight Dynamics of Airships with Application to the YEZ-2A. PhD thesis, College of Aeronautics, Cranfield University, 1990.
- [Hall 2002a] J. L. Hall, V. V. Kerzhanovich, J. A. Jones, J. A. Cutts, A. A. Yavrouian, A. Colozza, R. D. Lorenz. "Titan Airship Explorer", in *Proceedings of the 2002 IEEE Aerospace Conference*, IEEE, Big Sky, MT, March 2002.
- [Hall 2002b] J. L. Hall, A. Elfes, T. Spilker, V. Kerzhanovich, J. F. Montgomery. "Titan Aerobots: An Overview of Mission Scenarios and Required Autonomy Technologies". Whitepaper, JPL 2002.
- [Hall 2004] J. L. Hall, V. V. Kerzhanovich, A. H. Yavrouian, J. A. Jones, C.V. White, B. A. Dudik, G. A. Plett, J. Mennella and A. Elfes (2004). "An Aerobot For Global *In Situ* Exploration of Titan", 35th COSPAR Scientific Assembly, Paris, France, July 20-24, 2004.
- [Kerzhanovich 2002] V. V. Kerzhanovich, J. A. Cutts, H. W. Cooper, J. L. Hall et al. "Breakthrough in Mars Balloon Technology", in *Proceedings of the World Space Congress / 34th Scientific Assembly of the Committee on Space Research (COSPAR)*, Houston, TX, USA, October, 2002.
- [Kröplin 2002] B. Kröplin. "Solar Airship LOTTE". Technical Report, Institute for Statics and Dynamics of Aerospace Structures, University of Stuttgart, Germany, 2002.
- [Lorenz 2000] R. D. Lorenz. "Post-Cassini Exploration of Titan: Science Rationale and Mission Concepts". In *Journal of the British Interplanetary Society*, vol. 53, UK, 2000.
- [NASA 2003] Solar System Exploration. http://spacescience.nasa.gov/admin/divisions/se/SSE_Roadmap.pdf.
- [Payne 2004] J. Payne, S. S. Joshi. "6 Degree-of-Freedom Non-Linear Robotic Airship Model for Autonomous Control". Robotics, Autonomous Systems, and Controls Laboratory (RASCAL) Technical Report 040521, University of California, Davis, 21 May 2004.
- [Roumeliotis 2002] S. I. Roumeliotis, A. E. Johnson, and J. F. Montgomery. "Augmenting Inertial Navigation with Image-Based Motion Estimation". In *Proceedings of the 2002 IEEE International Conference on Robotics and Automation*, Washington, DC, 2002.
- [VEGA 1985] "Venus VEGA Mission Detailed Description", http://robotics.jpl.nasa.gov/tasks/aerobot/studies/vega_detail.html.